2

AN EXPERIMENTAL STUDY OF PLASMA STRUCTURE IN A SMALL RAILGUN

D. F. STAINSBY

MRL-R-1057

AR-005-136

MATERIALS RESEARCH LABORATORY

An Experimental Study of Plasma Structure in a Small Railgun

D.F. Stainsby

MRL Report
MRL-R-1057

Abstract

Miniature B-dot coils were used to probe the current in the plasma boundaries at both the positive and negative rails in a small railgun. Waveforms from a row of three coils at each rail were examined for evidence of the existence of time-ordered fine structure effects within the plasma boundary. No such order was detected. However, spatially correlated effects were observed and these were attributed to rapidly changing filamentary structure in the plasma. The polarity-reversal, or cross-over characteristics, of the B-dot waveforms showed anomalous features. Possible explanations are discussed. Evidence from rail damage is presented supporting the view that the rail-plasma boundary is associated with a number of complex processes and that localized irregularities in the B-dot waveforms should be expected.

Published by

DSTO Materials Research Laboratory
Cordite Avenue, Maribyrnong
Victoria, 3032 Australia

Telephone: (03) 319 3887
Fax: (03) 318 4536

AR No. 005-136

APPROVED FOR PUBLIC RELEASE

Contents

An Experimental Study of Plasma Structure in a Small Railgun

1. Introduction

Railgun modellers have consistently described the distribution of plasma-armature properties along the bore of a railgun by simple mathematical functions. Plasma parameters have usually been assumed to be constant over cross-sections perpendicular to the bore axis, although some authors have drawn attention to evidence that a more complex armature structure exists [1, 2, 3]. Armature voltages computed for practical systems [3, 4] are approximately one third of measured values. Marshall [3] postulated that the voltages occurring across rail-boundary arc-roots, or 'sub-arcs' as he preferred to call them, would explain the discrepancy between the theoretical and practical armature voltage. A voltage drop of approximately 60 V across the arc-roots at each rail, added to a 'bulk plasma' potential drop of similar value, would account for recorded voltages of 150 to 180 V.

Sub-arcs were visualised as localised and highly dynamic boundary effects which, in the railgun environment, generally moved along the bore axis relative to the bulk plasma. Such a supposition followed from examination of the arc-tracks observed on gun rails. Furthermore, the complexity of additional signals superimposed on basic B-dot waveforms in a number of gun firings was though to support the idea of a fine sub-arc structure.

To acquire information on the numbers and movement of the sub-arcs, a number of experiments were conducted. This report documents and interprets these experiments. It integrates observations, experiments and ideas from a large number of activities. Much of the assessment is of necessity qualitative. Firstly, an attempt was made to use high speed photography in conjunction with a transparent gun body [5, 6]. The bore was masked so that only a few millimetres along one rail interface was exposed. The attempt however was unsuccessful and was not pursued.

It was then considered that the most practical way to observe boundary sub-arc activity was to use miniature dB/dt (B-dot) probes positioned in the body just outside the bore close to the plane of the rail-face. Using assemblies of coils, data were collected from six firings of a small, injection-assisted railgun. (Injection had no significance for these tests).

This railgun had a 10 mm square bore with 16 mm × 5 mm copper-cadmium rails in a laminated polycarbonate body. Rail length was approximately 450 mm (see Fig. 1). The injection velocity was approximately 1300 m/s.

A further B-dot coil was used to provide data for obtaining the approximate speed of the plasma centroid past the array. This was sited in a conventional B-dot bore-centreline position 24 mm from the array centre, and closer to the muzzle as shown in Figure 1.

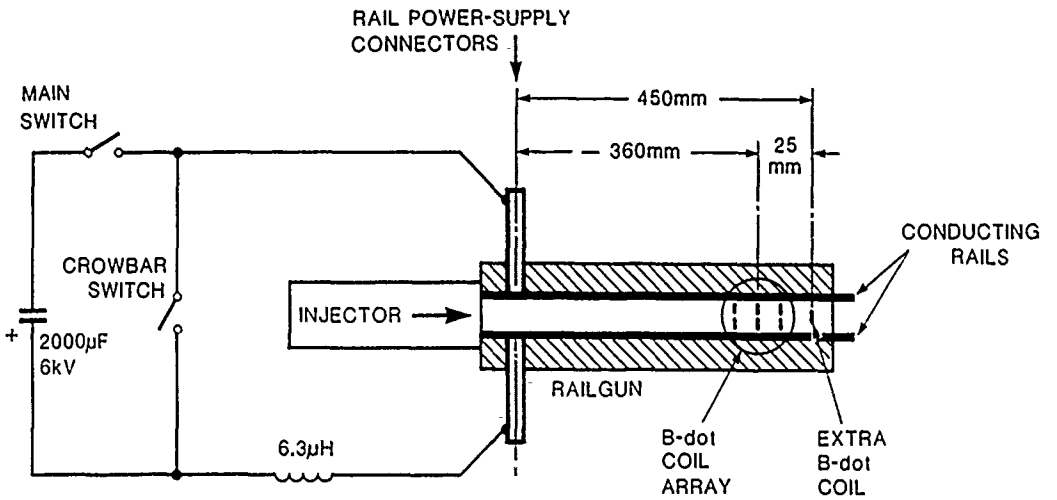

Figure 1 Basic gun showing coil locations.

2. The Coil Assembly

A single assembly, containing a number of individual coils, was found to offer many practical advantages. Firstly it ensured consistent alignment of coils, secondly it reduced machining and mounting effort required for individual coil sites, and finally it was convenient for gun assembly and instrumentation cabling.

To enhance coil-to-coil alignment, the coils were wound on rods which were then glued to grooves in the end of 16 mm diameter plastic tube. The leads from each coil were twisted and taken to coaxial connectors on a common block. The purpose of twisting the leads was to balance-out off-axis influences. The edge of the block, which was aligned with the coil axes, was used for alignment with the gun axis. Figure 2 shows the coil array location relative to rails and bore. The number of coils in the array varied from experiment to experiment. Details are given later.

As can be seen in the figure, a flat-bottom hole was machined to within 4 mm of the rail edges, giving a coil centreline to bore centreline separation of approximately 13 mm. This was as close to the rail edges as was believed practicable without too great a risk of cracking the railgun body during firing. No cracking occurred during the firings.

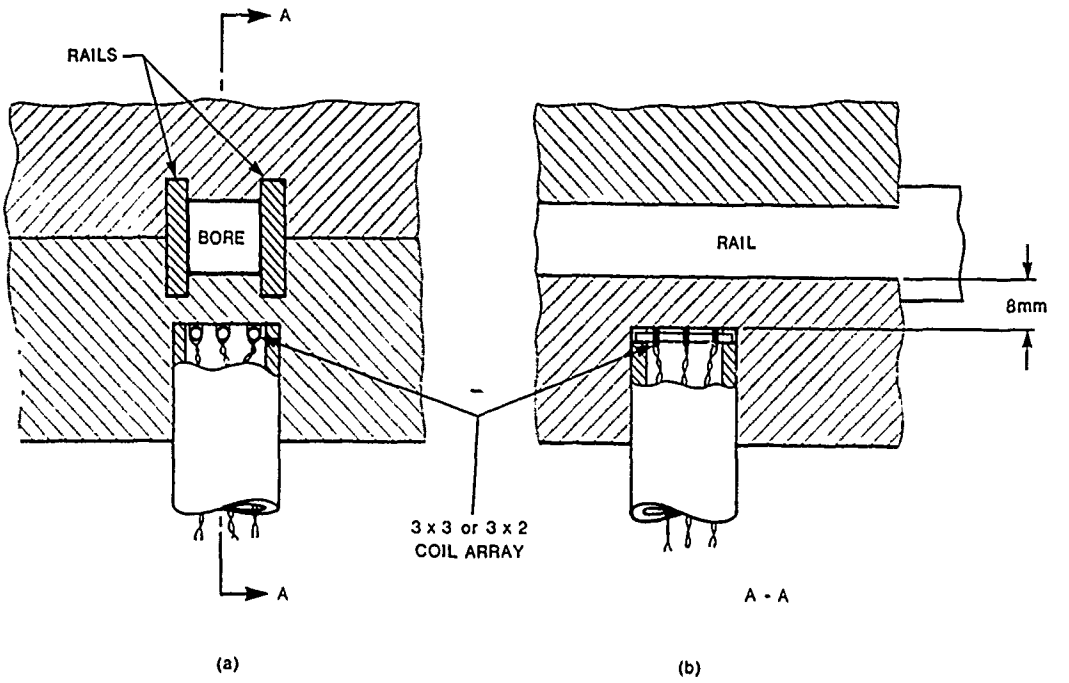

Figure 2 Coil array location relative to rails.

The probe assembly was installed at a position 360 mm from the centreline of the rail current-connectors, firstly so that it would be in a region where experience had shown that arc tracks were usually well established, and secondly so that it would not clash with bolt-hole positions in the gun-body.

Three assemblies were used during the tests. The first of these was a 3×3 array, with edge row centrelines approximately 1 mm inside the rail-face plane, and approximately 3.5 mm coil spacings (Fig. 3). Coil rows were equally spaced. Each coil consisted of 15 turns, with a measured inductance of approximately 0.55 μH.

To ensure that coil-connectors had been correctly identified, coil inductance was measured at each connector in turn, while a ferrite tipped probe was moved from coil to coil. The proximity of the ferrite to a particular coil increased the inductance, and so coil-connector association could be easily tested.

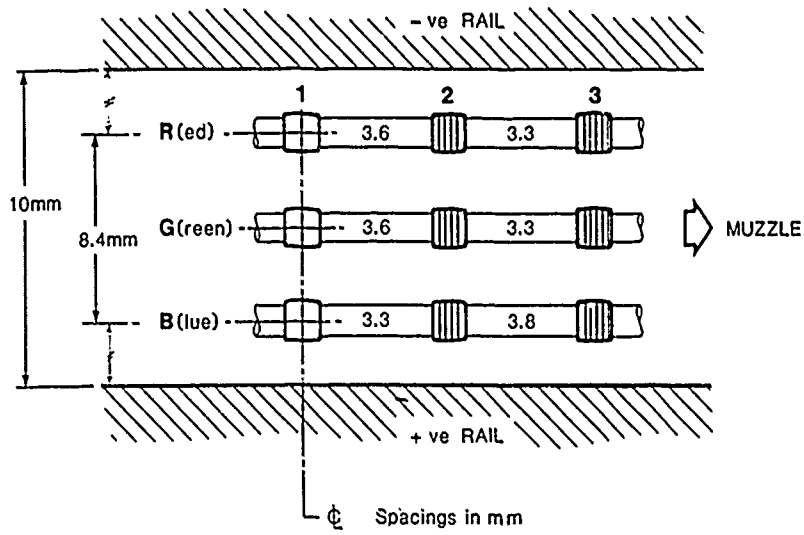

Figure 3 Array coil identification and separations for the first experiment, SUBAC.

3. Recorders and Timing

Three twin-channel and three single-channel recorders were used for monitoring the array outputs. A twin-channel recorder was allocated to two coils in each row to reduce timing uncertainties for motion along the bore direction. These paired channels are identified in the tabulations of results. The analog-to-digital convertors within a twin-channel recorder were clocked synchronously, eliminating timing uncertainty, but recorder-to-recorder relative timing was established by the triggering, which for all experiments was derived from a common source. Figure 4 shows the set-up for experimental timing control. All recorders were of 8-bit design. Based on earlier experimentation, this was considered adequate provided recorder sensitivities were set appropriately.

The spread of timing-delay over all optical trigger-links was measured to be 0.2 μs. Recorder timing uncertainties are specified to be appreciably smaller than this. The maximum available recorder-sampling-rate was 10 MHz, but 5 MHz was used for the early tests. With an expected array traverse time of approximately 4 μs, this was considered marginal but adequate for discriminating significant differences in times-of-arrival of the centroid at coil sites, and for resolving significant waveform perturbations arising from sub-arc activity.

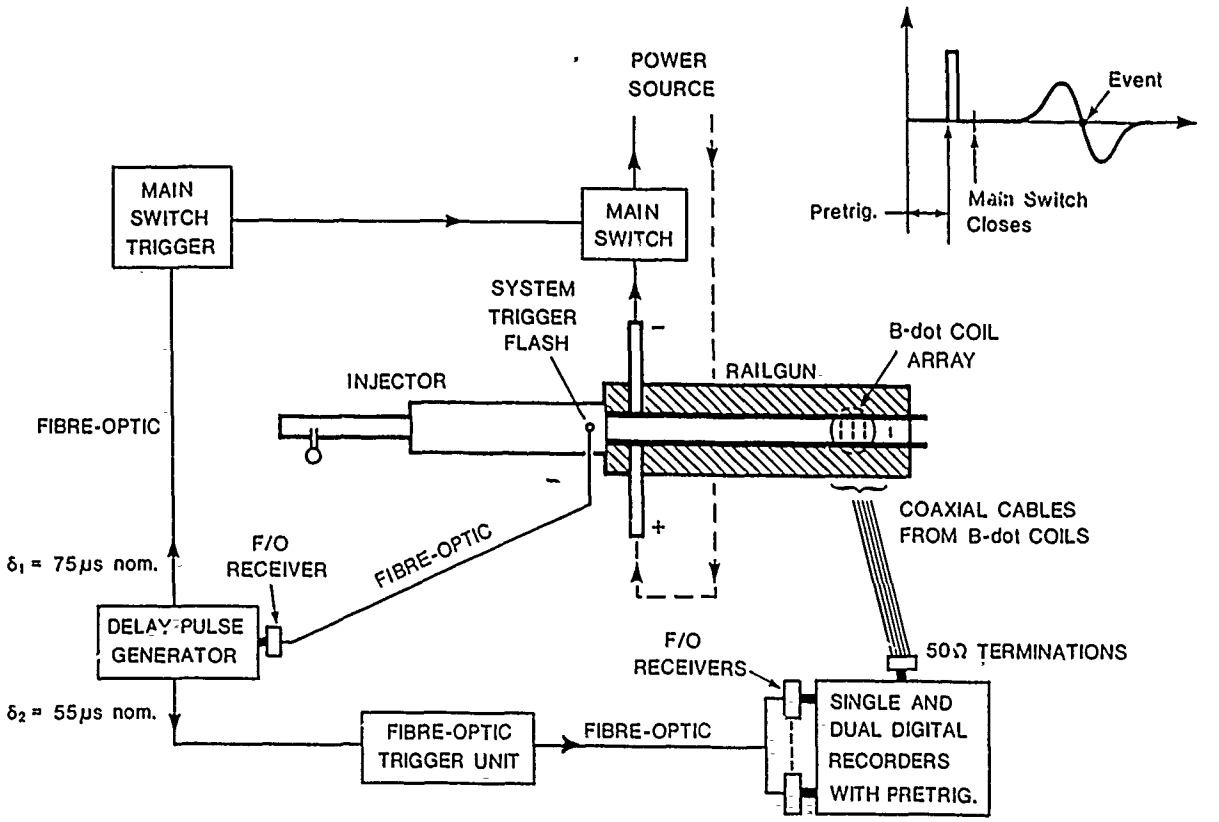

Figure 4 Instrument timing arrangement.

4. The SUBAC Experiments

SUBAC was the acronym given to the set of four experiments specifically directed at investigation of sub-arcs. In subsequent experiments, sub-arc experiments were incidental to the primary purpose of the firings. Of the four firings conducted using the 3×3 array of Figure 3, three produced useful data sets. SUBAC 1 fired without electrical propulsion. For SUBAC 2, eight of the nine waveforms were clipped as a result of recorder overload. Consequently the only experiments discussed in detail are the two identified as SUBAC 3 and 4.

4.1 Results of SUBAC

Waveforms from SUBAC displayed appreciation variation in detail. Examples from SUBAC 4 are shown in Figure 5. Examination of the B-dot waveforms gathered from the nine coils in the array led to the following observations:

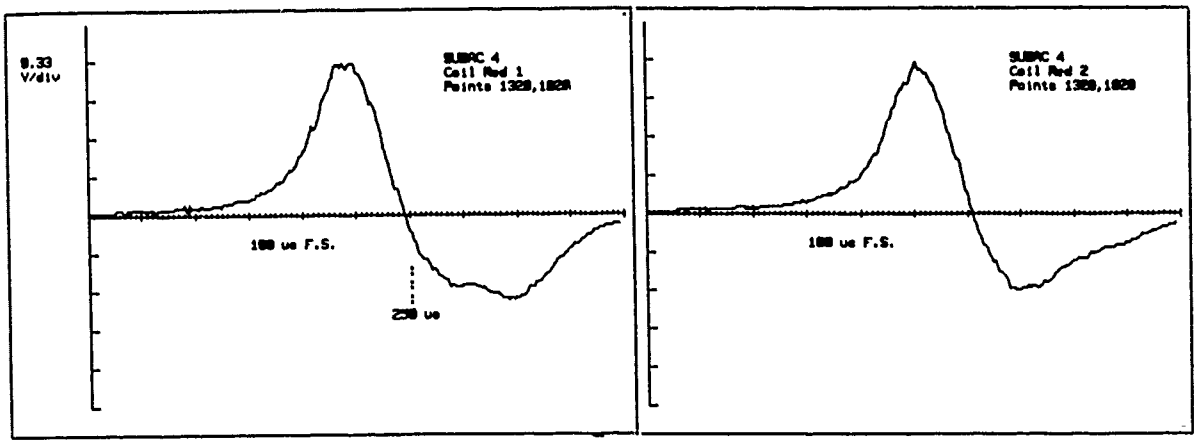

(a) (b)

Negative-rail B-dot waveforms for SUBAC 4

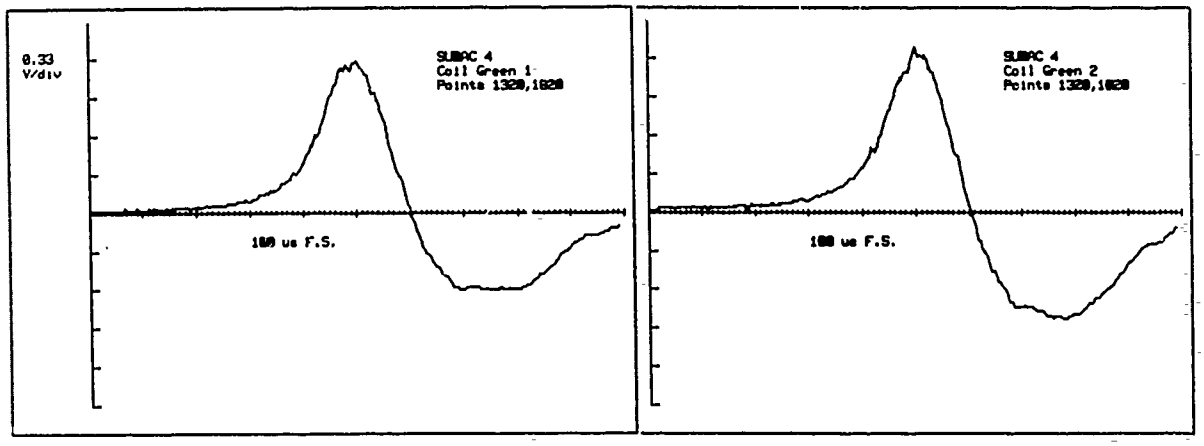

(c) (d)

Centreline B-dot waveforms for SUBAC 4

Figure 5 Representative B-dot waveforms for negative rail (R) and centreline (G) coils.

1. Each waveform showed fine or coarse variations from the classical smooth B-dot S-curves [7]. Such features could possibly have been associated with sub-arc activity or some irregularity of current distribution within the plasma body. Note for example in Figure 5 the fine variations around the first peak, in contrast with the coarser variations around the second peak of B-dot, e.g. (a) and (d).

2. Features on one waveform (e.g. G1) from within a line of coils (Green) could not be confidently correlated with features on waveforms from the other two coils in the same line (i.e. G2 and G3). Hence there was no basis for investigating relative movement of

arcs along the bore direction within the plasma, i.e. there was no feature which could be clearly seen to be shifting.

3. Centreline coils in the array produced the same general waveform features as the coils near the rail edges. However for SUBAC 4 some waveform sets were very similar. This is shown in the remarkably similar perturbations around the first-peaks for the waveform sets R and G in Figure 5(e), i.e. R_1 looks like G_1, R_2 looks like G_2, R_3 looks like G_3. This would lead one to consider that the phenomena causing the fine perturbations may not have been highly rail-localised, or that coil to plasma separation was too great to discriminate side to side effects.

4. For SUBAC 4, consider again the red and green coil sets of Figure 5(e). Since the two rows of coils R and G gave an almost identical pattern of change (around the first peak) as the plasma front progressed from column 1 to column 3, it seems probably that the waveform change does reflect a change within the plasma front. It is unlikely that spurious influences could produce such a uniform result, considering the hand built array construction, and the coil to coil variation likely to result

5. Although waveforms had features in common, considered in total each waveform was unique, supporting the view that the plasma was rapidly changing.

Analysis of the B-dot data for zero cross-over times disclosed interesting values of the coil-to-coil time increments. It was expected that reasonably uniform time-steps would be recorded, consistent with the image of a smoothly progressing and slowly changing plasma. A simple interpretation of the data obtained, however, could be that the plasma was experiencing significant changes in current distribution even over the short span of the array.

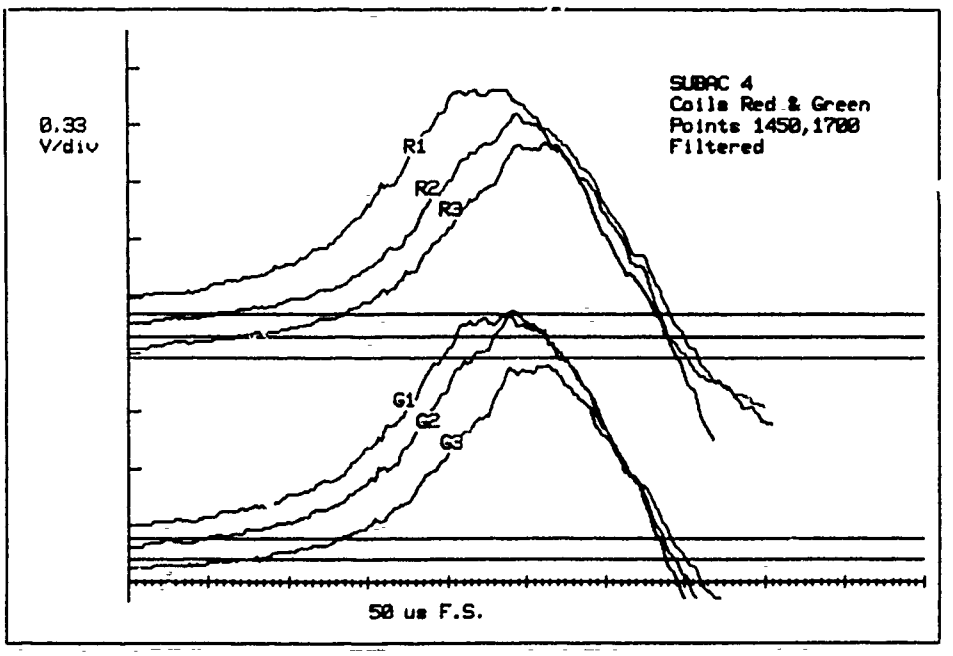

Figure 5(e) *B-dot first-peaks expanded and baselines offset to highlight coil row-and-column waveform similarities for SUBAC 4. The Blue coil row showed similar trends.*

Table 1 presents these data for SUBAC 3 and SUBAC 4. Timing is normalised to the earliest cross-over point for the set of coils.

Table 1 Relative time of arrival of the plasma centroid at individual coil sites for SUBAC

B-dot Coil Site			Normalised B-dot Cross-over Time (μs)	
Location	Name	Recorder Type & No.	SUBAC 3 (5 kV)	SUBAC 4 (6 kV)
Neg. rail	R1		0	0
Neg. rail	R2	X	1.8	1.2
Neg. Rail	R3	X	1.6	0.8
Central	G1		0.9	0.4
Central	G2	XX	2.7	1.0
Central	G3	XX	2.6	1.3
Pos. rail	B1	XXX	3.9	2.4
Pos. rail	B2	XXX	3.6	1.8
Pos. rail	B3		3.2	1.8

* Twin-channel recorders are shown as X, XX, or XXX. Unmarked indicates a single-channel recorder.

Note from Figure 3, uneven coil spacing for the B(lue) set.

The data, if valid, points to the existence of a plasma with a centroid which is sometimes stationary, and which sometimes moves backwards with respect to the bulk plasma. Unexpected timing data were evident even on twin channels where potential problems of relative timing did not arise. With an average plasma centroid speed over 25 mm to the extra B-dot coil of 1.7 km/s, an array traverse time of at least 4 μs would have been expected. Only the incremental times from R1 to R2 (negative rail) and from G1 to G2 (centre) (SUBAC 3) gave credible though excessive bulk-plasma velocities. Data for the positive rail coils was the least convincing for both shots. Positive and negative rail coils exhibited similar incremental behaviour for both shots. While it is interesting to contemplate the possibility of a plasma centroid standing still for several microseconds, or even jittering backwards while the bulk plasma (and projectile) continues to move forward, it would seem unlikely that the plasma would exhibit the same behaviour so closely at the same location on separate shots. Even incorrect coil identification would not have accounted for the above anomalies. The time-of-cross-over data must therefore be treated with caution.

4.2 Discussion of SUBAC

Although interesting observations were made on the basis of waveform data, anomalies in the time-of-cross-over data cast uncertainty on overall data validity. An explanation of the timing anomalies could be that the waveforms had been modified by some systematic effect such as interference from the rail current. It was accepted that this set of coil windings was

not completely suitable for the type of application, and a new set was subsequently made. The subject of interference is pursued in some detail in the final discussion.

5. The RIPAL Experiments

A second coil set without the centre row was used in another MRL railgun experiment, the two shots being identified as RIPAL 1 and 2. The rails for this experiment contained 5 mm wide aluminium inserts across the rail faces. There were two inserts in each rail. More detail on that aspect of the experiment is given elsewhere [7]. The coil details are shown in Figure 6.

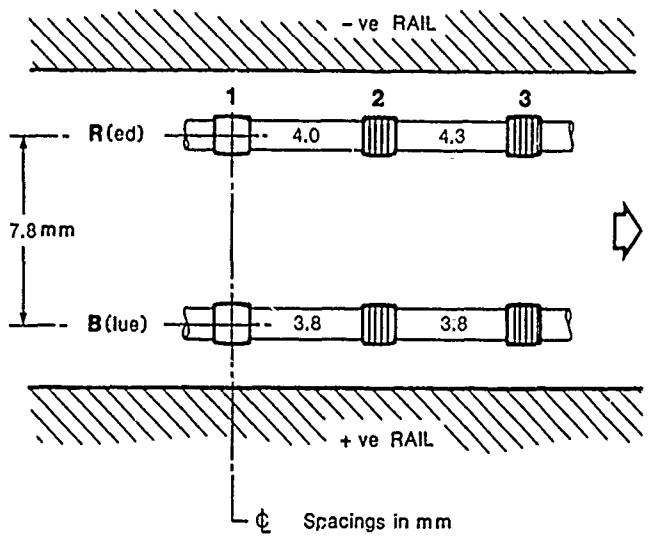

Figure 6 Array data for the Red and Blue rows.

For these experiments coil spacings were increased, the coils were more compact, more carefully wound and the locations were better defined. The assembly had a slight offset (0.5 mm) towards the negative rail. However it was felt that the effect was not sufficient to detract from the coil-set's potential to discriminate the effects under investigations. Inductance of the 11 turn coils was 1.4 μH.

To eliminate residual uncertainty about relative timing between recorders, the centre coil in each row was made common to both the first coil and second coil recorders. In the following tabulation the duplicated coil channel is identified with prefix A.

Sampling rate was increased for these tests, giving a sampling interval of 0.1 μs.

5.1 Results of RIPAL

The interconnection of coils proved, for the most part, to be not a particularly satisfactory arrangement, as the inter-recorder connection caused mistriggering and loss of data. The record sets are therefore incomplete.

Plots of representative waveforms are given in Figure 7.

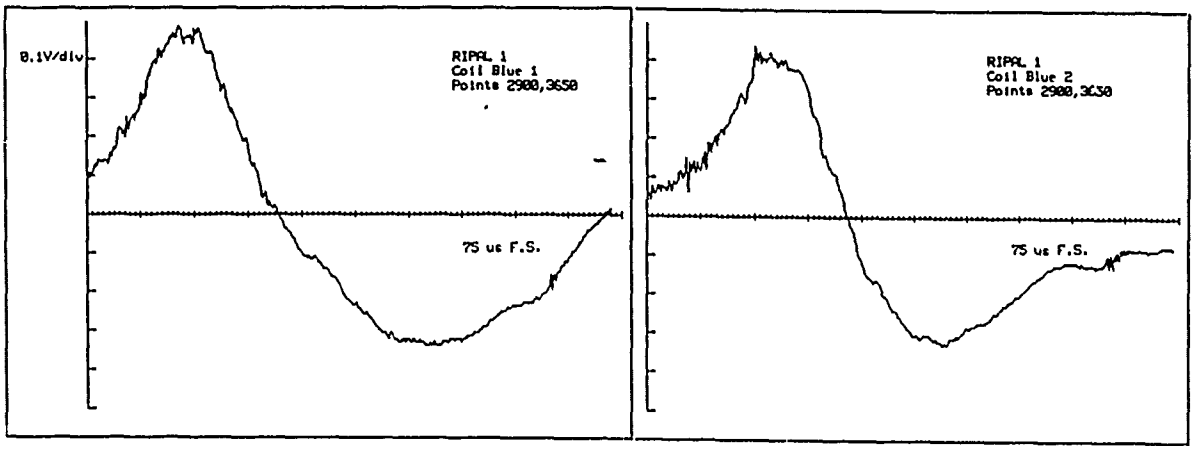

(a) Coil B1, RIPAL 1

(b) Coil B2, RIPAL 1

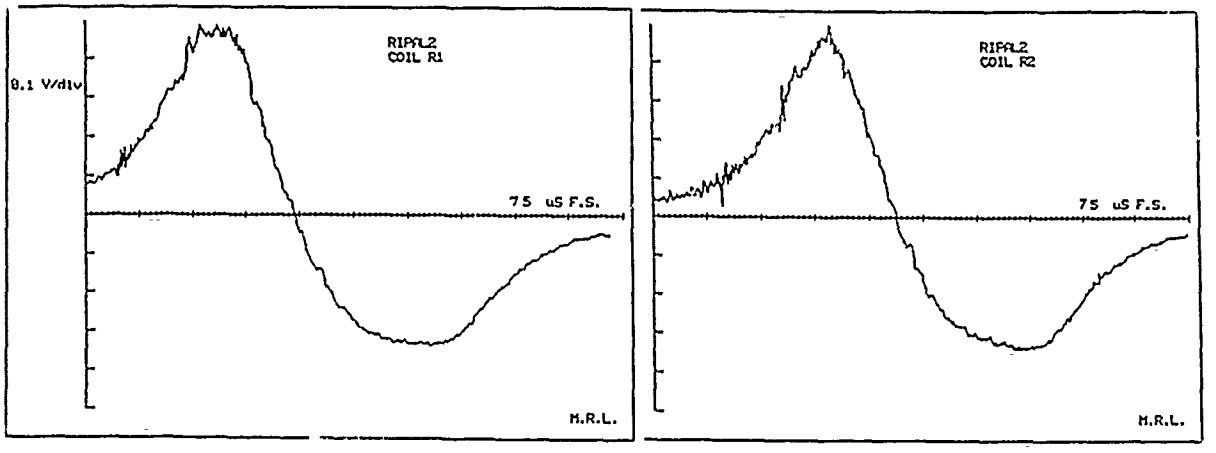

(c) Coil R1, RIPAL 2

(d) Coil R2, RIPAL 2

Figure 7 *Some B-dot waveforms for RIPAL.*

(a) and (b): RIPAL 1 positive rail coils.
(c) and (d): RIPAL 2 negative rail coils.

a, b, c, d time axes do not have the same time origin.

All waveforms exhibited a noise-like structure during the first half of the B-dot S-shaped waveform. However, there was little similarity in the fine detail of the waveforms. The second half was comparatively smooth, particularly for the RIPAL 2 experiment.

Data sets for the positive rail were appreciably noisier than those for the negative rail. This effect could indicate either that the set of coils monitoring the positive-rail all had poorer noise rejection than their counterparts, or that a real difference in plasma behaviour at the rails existed.

Once again, there were B-dot waveform cross-over anomalies. Relative times of arrival of the plasma centroid are shown in Table 2.

Table 2 **Relative time of arrival of the plasma centroid at individual coil sites for RIPAL**

B-dot Coil Site			Normalised B-dot Cross-over Time (μs)		
Location	Name	Recorder I.D.	RIPAL 1		RIPAL 2
Neg. rail	R1	X	0	- reference -	0
Neg. rail	R2	X	1.8		1.3
Neg. rail	AR2	XX	-		1.4
Neg. rail	R3	XX	-		4.9
Pos. rail	B1	XXX	0.9		-
Pos. rail	B2	XXX	2.2		-
Pos. rail	AB2	XXXX	2.3		3.5
Pos. rail	B3	XXXX	2.4		1.0

* X, XX, XXX and XXXX were twin-channel recorders

Only the negative rail coil triplet gave sensible values, resulting in an estimated 1.7 km/s for the average velocity over 8.3 mm, though the intermediate incremental values are widely different. Again the positive rail set gave the least convincing results, particularly for RIPAL 2 with a large negative time increment for the transition coil-AB2 to coil-B3. These discrepancies cannot be accounted for by instrument timing uncertainties.

5.2 Discussion of RIPAL

This second coil set gave figures for the plasma velocity which were only slightly more sensible than the set for the earlier SUBAC shots, despite considerable improvement in coil construction. The apparent time-of-arrival of the plasma at the RIPAL 2 coil-B3 appeared to be 3 to 4 μs in error (assuming a plasma velocity of 1.7 km/s). On this basis, any attempt to compare times-of-arrival of perturbations would have been futile.

The apparent deterioration in behaviour for the B2/AB2 to B3 transition for the RIPAL 2 shot compared with RIPAL 1 was difficult to understand, unless it was accepted that there was a real difference at the positive boundary in the two shots. Coil set-up was unchanged, and the gun electrical parameters were unchanged. Exit velocities for these two shots were very similar at 1790 and 1780 m/s respectively.

These two experiments produced similar waveforms to the earlier SUBAC shots. However, the first peaks of the B-dot waveforms were noticeably noisier for the RIPAL shots. As was the case for the SUBAC data, the noise on the array coils did not appear to have significant features that could be correlated coil-to-coil.

6. The RIPLAM Experiment

Further tests were undertaken in another MRL experiment identified by the acronym RIPLAM. The rails for this experiment had been milled lengthwise to generate three channels which were filled with an insulating material. More detail on that aspect of the experiment is given elsewhere [7]. Details of the coil set are shown in Figure 8.

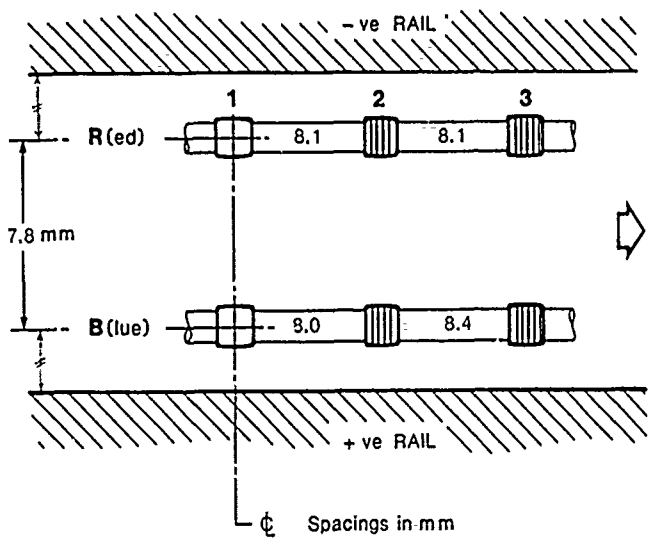

Figure 8 Array data for the Red and Blue rows.

For these tests, the coil separation was doubled to 8 mm to minimise the proportional contribution of timing errors introduced by any coil inadequacies which might exist. As the coil formers then extended beyond the cylindrical hole, slots were milled into the polycarbonate body. This arrangement also aided array alignment.

6.1 Results and Discussion

A record was obtained for each of the six array coils, as presented in Figure 9.

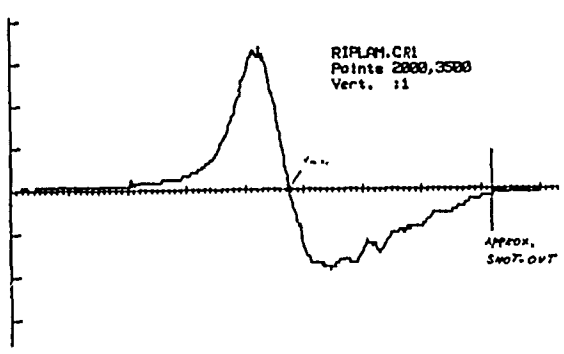

(a) R1

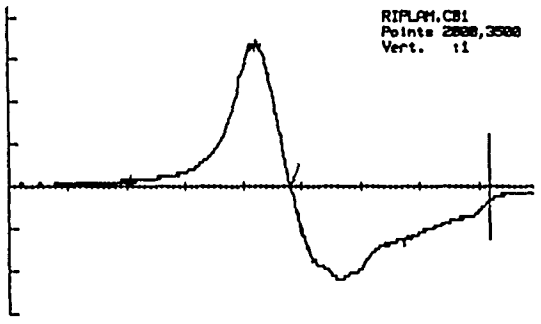

(d) B1

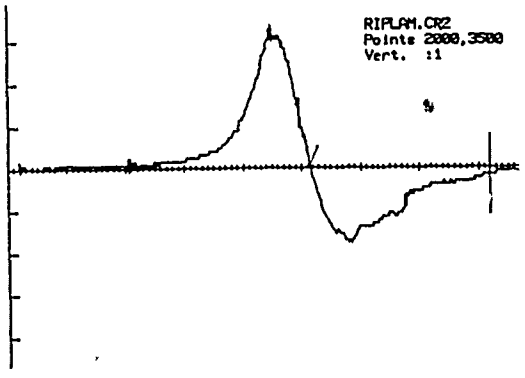

(b) R2

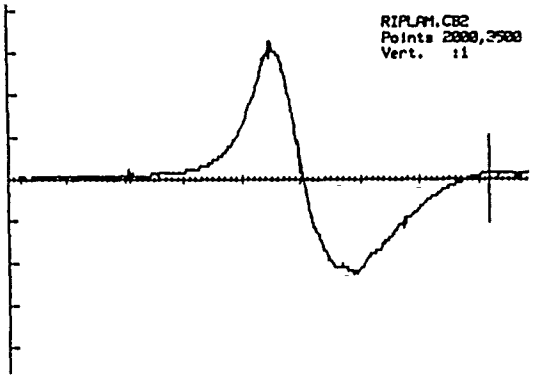

(e) B2

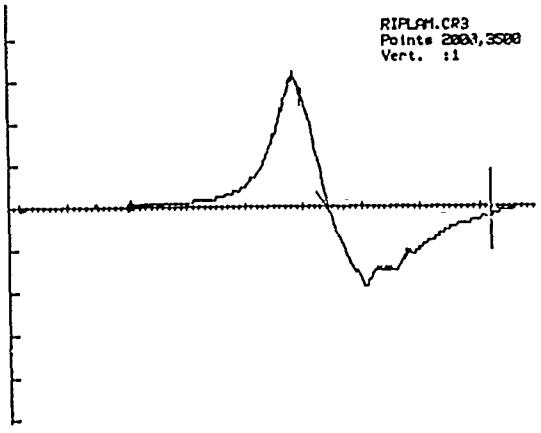

(c) R3

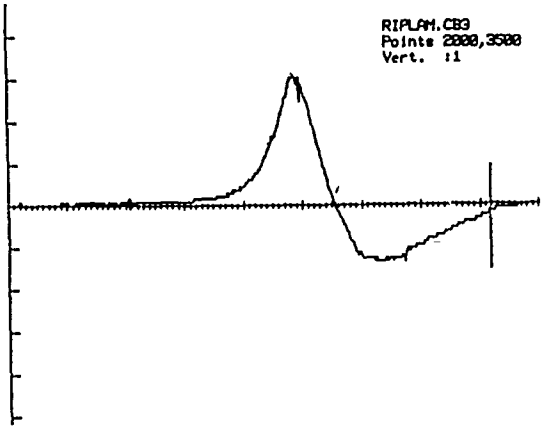

(f) B3

Figure 9 *B-dot waveforms for RIPLAM. Scales : 15 μs/major div, 0.25 V/div*

(a) to (c): Negative rail B-dot waveforms.
(d) to (f): Positive rail B-dot waveforms.

All waveforms showed fine structure (or noise) around the first peak, as was observed in the earlier experiments. Some noise was evident in the second half. Structure detail in the second half of the waveforms was different for positive and negative rail coil-sets, being noticeably coarser for the negative rail set. This suggested a different current distribution in the plasma tail at each rail for this particular firing and rail-set. No such obvious pattern was observed on either of the earlier experimental sets.

In order to show some of the first peak detail, the waveforms are presented again on an expanded time scale in Figure 10. It can be seen that there are some features which are common across two or more coils, with one feature traceable across all. Since the only significant noise source was the plasma arc itself, it could be postulated that each occurrence corresponded to a significant arc strike or extinction. All such noticeable features were ahead of, or just after, the B-dot cross-over, and are considered to be mainly associated with the leading part of the plasma.

Referring to Figure 10 it must be noted also that, as for some of the SUBAC 4 waveforms, there is a clear likeness of coil column pairs in the vicinity of the first B-dot peak. Furthermore, the character of the first peak changes in progressing from the first column to the third column.

Relative cross-over times for the RIPLAM B-dot waveforms were evaluated, and are given in Table 3.

Table 3 **Relative time of arrival of the plasma centroid at individual coil sites for RIPLAM**

B-dot Coil Site			Normalised Cross-over Time (μs)	Time Increment (μs)	Coil/Coil Velocity (km/s)	Overall Velocity (km/s)
Location	Name	Recorder Pairs*				
Neg. rail	R1	X	1.0			
				6.0	1.4	
Neg. rail	R2	X	7.0			1.6
				4.2	1.9	
Neg. rail	R3	XXX	11.2			
Pos. rail	B1	XX	ref - 0			
				3.5	2.3	
Pos. rail	B2	XX	3.5			1.3
				9.4	0.89	
Pos. rail	B3	XXX	12.9			

* X, XX and XXX are twin-channel recorders.

It can be seen that, with the increased array length of 16 mm, all outputs were at least in a 'sensible' progression. Timing anomalies however persisted, discrepancies being far in excess of recorder errors. The negative rail set gave the more realistic average plasma velocity, and more uniform coil-to-coil time increments. The ratio of the time increments for the positive-rail coils was 2.7:1 which as for SUBAC seemed improbable.

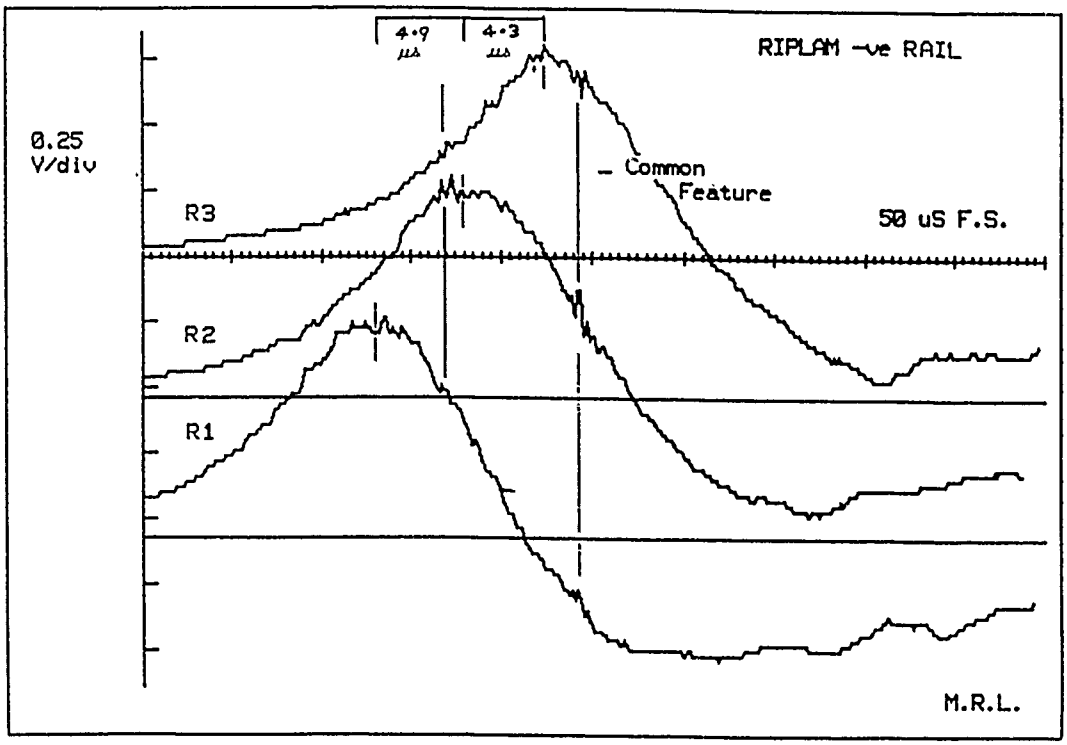

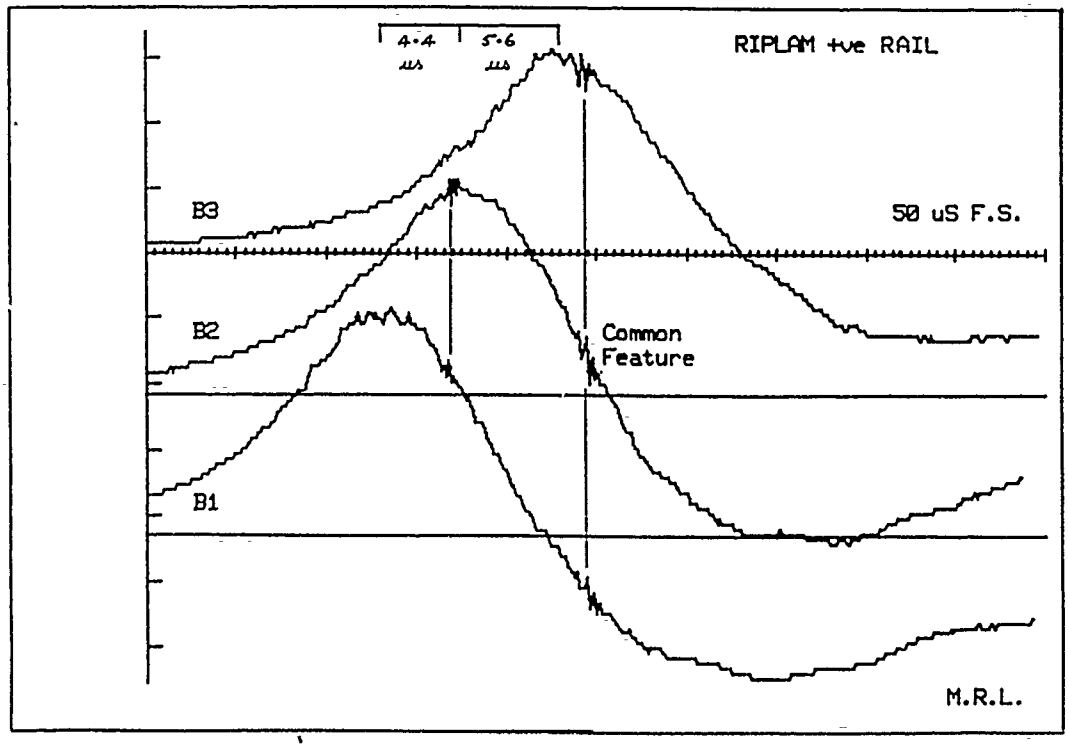

Figure 10 *Coil data for experiment RIPLAM expanded for coil-to-coil feature correlation and first-peak times-of-arrival*

Rail damage caused by the plasma was examined to give additional insights into the anomalies of timing and waveform variation over the array. This is discussed below.

7. Rail Damage Evidence

As noted earlier, the coil array was deliberately located at a position along the barrel where gross damage did not occur and where it was usual to see many arc tracks on the rails. Heavily damaged tracks can reasonably be taken to indicate those regions carrying the heaviest currents, and so are indicative of the greatest influences on flux waveform measurement close to the plasma. B-dot coils are not only sensitive to current amplitude changes but also to current (or arc-filament)-velocity changes, such as might be caused by arcs striking, jumping, or being extinguished. With this possibility in mind, photographs of some of the rails used in these experiments were examined. Figures 11 a, b, c, d show photographs of a section of the rails close to the array site from SUBAC 3 and 4, and RIPAL 1 and 2 respectively.

It is readily seen that although there are features common to these four rail sets, the damage detail is specific to each rail and to each shot (and sometimes markedly so), as shown in the examples of SUBAC 3 (Fig. 11(a)) and SUBAC 4 (Fig. 11(b)). SUBAC 3 produced a much coarser pattern of damage on the negative rail than on the positive rail with heavily damaged paths (or combination of paths) petering out, and new concentrations becoming evident. On the SUBAC 4 rails, the pattern was somewhat reversed, fine and regularly patterned tracks being conspicuous on the negative rail, and with signs also of divergence of tracks away from the bore centreline. Damage on the positive rail was interesting both in its contrast with that on the other rail, and in the impression that the current distribution across the rail had become more uniform with plasma movement to the right. Numerous fine meandering tracks were noted on the negative rail of SUBAC 3 (right-hand-end). Their relative lack of direction could suggest that they were not associated with the high-velocity main body of the plasma.

Figures 11(c) and (d) show rail sections from RIPAL 1 and 2. On the RIPAL 1 rails the damage was reasonably similar on both rails, with evidence of a trend towards concentration of current to the centre of the bore, with movement to the right. Relatively unscathed bore surface (near the bore edge) can easily be seen.

RIPAL 2 rails (Fig. 11(d)) show different patterns again. On the negative rail, the surface area occupied by arc-tracks reduces with movement to the right. The positive rail damage suggests concentration of the plasma current just below the bore centreline right across the record on this rail. It seems that very little current would have been coming from the lower portion (say 20%) of the bore over this region. Many short and angled tracks are evident on both rails of the RIPAL records, as well as the SUBAC records.

The rail damage in the region of the array was characterised by different arc patterns of movement and concentrations not only on each shot, but also on each rail, with changes occurring over short distances. There can be little doubt that such variations at the rail faces would have been reflected to some extent in the waveforms registered by the coils of the array, although averaging through spatial separation of bore and array would have tempered any such effects.

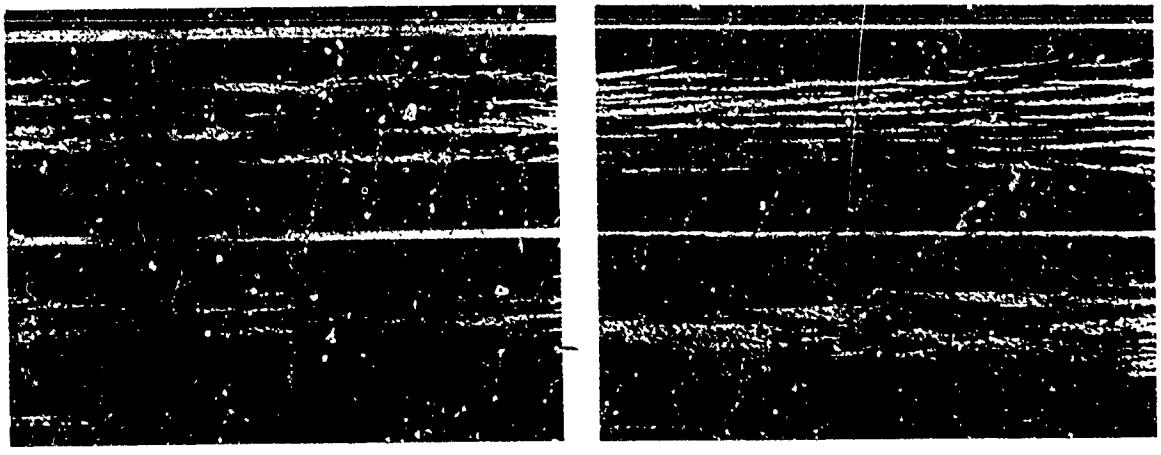

MUZZLE

(a) Rails from Shot SUBAC 3

(b) Rails from Shot SUBAC 4

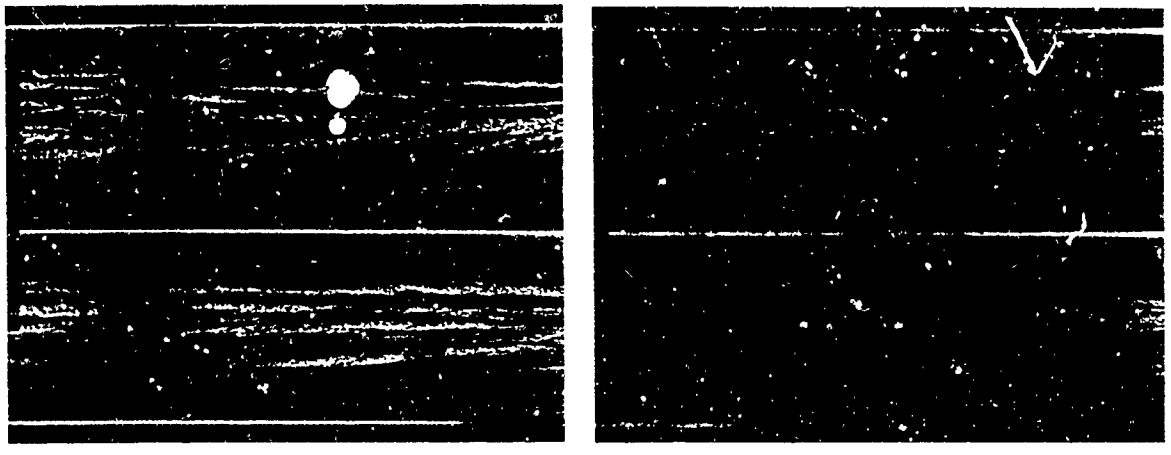

MUZZLE

(c) Rails from Shot RIPAL 1

(d) Rails from Shot RIPAL 2

Figure 11 *Arc rail-damage near the location of the coil array. Rails are shown folded out. In all sets the lower rail is positive.*

8. Information from Streak Photography

It is interesting to note that the rail damage variations discussed above occurred in an interval during the firing cycle when the plasma would seem, from measurements, to have been very stable. Figure 12 shows the photographic streak record of RIPAL 2 with the coil-array location marked. The print was processed to suppress low intensity effects. This streak is typical of the streak records for the shots presented here. It should be noted that obturation was excellent for all these firings.

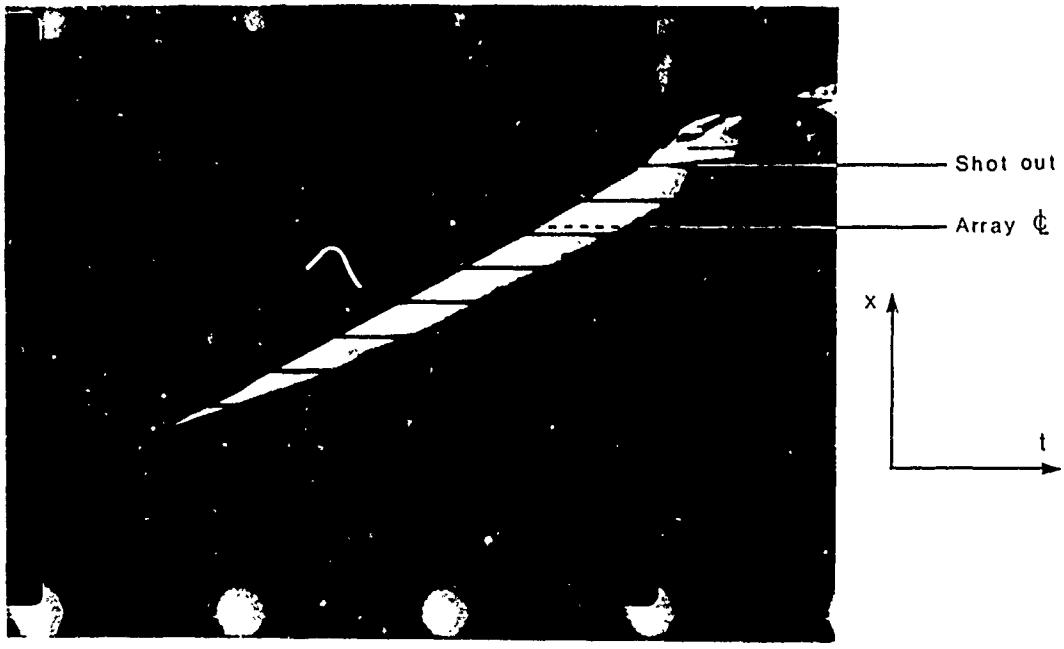

Figure 12 *Typical streak record showing the array location (RIPAL 2). Displacement markers are at 50 mm separation. Time markers are at 100 μs intervals.*

Other data relevant to the condition of the plasma during the recording interval are shown in Table 4.

Table 4 **Basic plasma data at array site**

Parameter		Value
Plasma Current		75 kA
Current Rate-of-change		-0.1 kA/μs
Plasma Length	(Streak)	7 cm
	(B-dot)	5 cm
Plasma-Front Speed		1.7 km/s

9. Discussion

The experiments described above required recording-instrumentation with the capability to:

1. resolve perturbations on the basic B-dot waveforms, and

2. resolve significant timing shifts of the perturbations, relative to the baseline cross-over, which occurred as the plasma progressed along the row of three coils.

For the information to be simply interpreted it was essential for the outputs of the various sensors to be adequately immune from corruption by other environmental influences. While the equipment provided the basic capability to satisfy amplitude discrimination and timing demands, distortion of a waveform could negate this by modifying the base-line cross-over, and thereby falsifying timing information.

In retrospect, some evidence bearing on this possibility is available. One misfire, SUBAC 1, in which there was a total discharge of the electrical energy across the muzzle, occurred with the coil array in position. Thus the array would have experienced the whole gun discharge rail-current pulse. Sample coil outputs are shown in Figure 13.

For a perfectly wound B-dot coil with its core axis perfectly aligned with the gun bore, there should be no response to idealised rail current changes. When a gun misfires and discharges across the muzzle instead of behind the projectile, the rail current time profile is close to that for a normal firing, being controlled initially by L and C, then L after crowbar. However, because the rail current here uses the full length of the rails from time-zero (cf the sliding short circuit), the coil array experiences flux with the same time profile as the rail current. Any B-dot response due to undesired cross-axis sensitivity would have the time profile of the time derivative of the rail current, i.e. approximately a single positive half cosine followed by a constant negative value corresponding to the current ramp-down after crowbar. The cross axis effect from rail current would therefore be greatest shortly after 'shot' start. This effect is certainly evident for B1 (Fig. 13), and less so for R3.

The coil array would not only experience rail current flux changes (cross axis), but also on-axis flux changes arising from the muzzle arc which bends away from the gun muzzle because of the rail current flux. Since the arc did not pass the array, the time profile of B was the same as for the rail current, but of considerably less magnitude at the array because of spatial separation from the muzzle. The array response would again be predominantly one-sided. The responses were in fact single sided, lending support to the above analysis.

Referring to Figure 13 again, the R2 and G3 signals are typical. R3 and B1 registered the largest response. Peak spurious signals recorded were approximately 5% of peak B-dot levels. One record for a shorted coil gave only spikes, showing that the cabling and recorder were not picking up significant interference. This would seem at first to indicate that the cross-axis insensitivity of the coils was adequate. But in reality, at the time of plasma B-dot cross-over, interference from rail current is at its maximum.

Consider the railgun simplification of Figure 14, i.e. parallel rails with a shorting bar. If the maximum flux on the gun centre-line due to rail current is B, the flux on the centre-line at the short is B/2. This translates to an inflection point on the (B, t) curve as seen at a stationary point on the gun axis, if the short were to slide past the point. The corresponding B-dot curve is as shown.

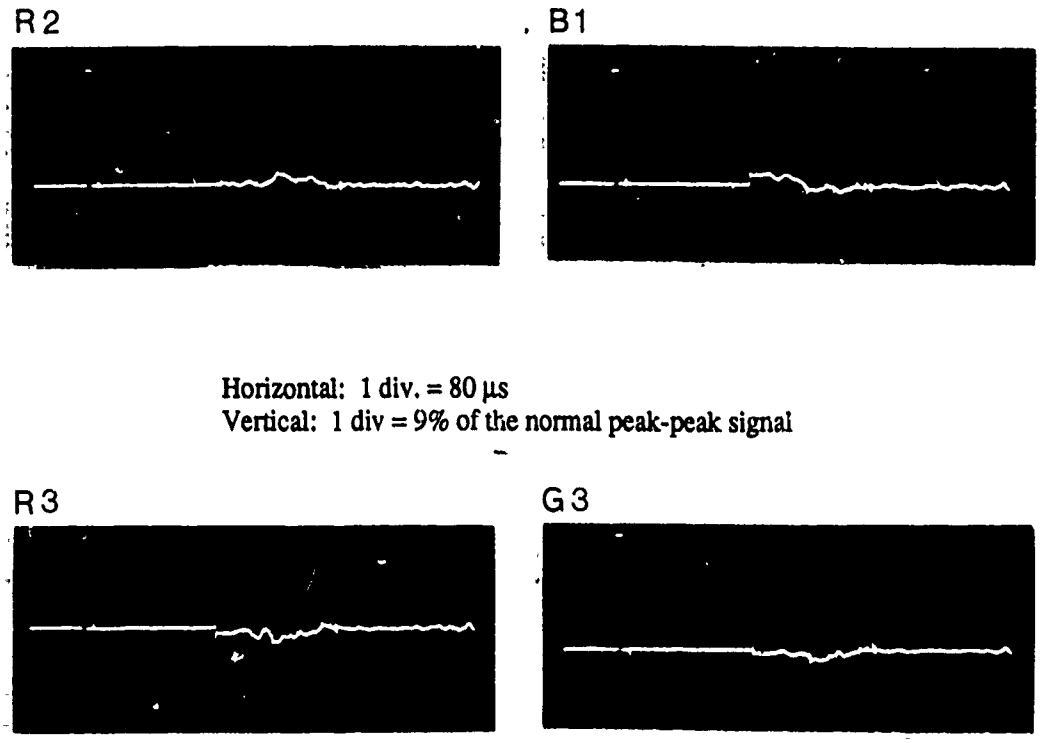

Figure 13 Some SUBAC array outputs for muzzle-arc only.

To a first approximation then, rail current in a firing induces peak cross-axis B-dot voltage as the plasma centroid passes the conventional B-dot coil site. At that time, the plasma induced B-dot response is approximately zero. This is the worst possible combination for measurement of the time of cross-over of the B-dot waveform, i.e. the signal to noise ratio is very poor at the most critical time. Looking again at the R3 and B1 responses of Figure 13, it will be seen that they are of opposite sign. This is consistent with the 'error' pattern for those two channels in Table 1, assuming the coils were wound the same way (as intended). Thus for both SUBACs 3 and 4, R3 has given a lower than expected time, while B1 has given a higher than expected figure. The relative error magnitudes are also roughly matched.

If in fact rail-current was the main source of interference, the signal to noise ratio would be considerably improved at the peak values of the B-dot waveform when the interference would also be less. One would therefore expect to derive more reliable time-increments between first peaks (say) than between cross-overs, although the definition of peak is not as clear as cross-over.

Pursuing this idea of measuring relative-time-of-arrival from first-peak data rather than baseline cross-over times, a reappraisal was made of the poor positive-rail RIPAL 2 data. This gave a coil-to-coil transit time for B1 to B2 of 4.5 μs compared with the cross-over figure of 1.3 μs, reducing the apparent plasma velocity from a high and unlikely 2.9 km/s to a low 840 m/s which is equally unlikely. Using the same approach on the positive-rail B2 to B3 coil data of both RIPAL 1 and RIPAL 2 gave no variation of transit time compared with the figures from cross-over times. Although this is the ideal result, i.e. no change, the result was surprising considering the implication. The negative transit time predicted by this coil pair for both experiments was not a credible result.

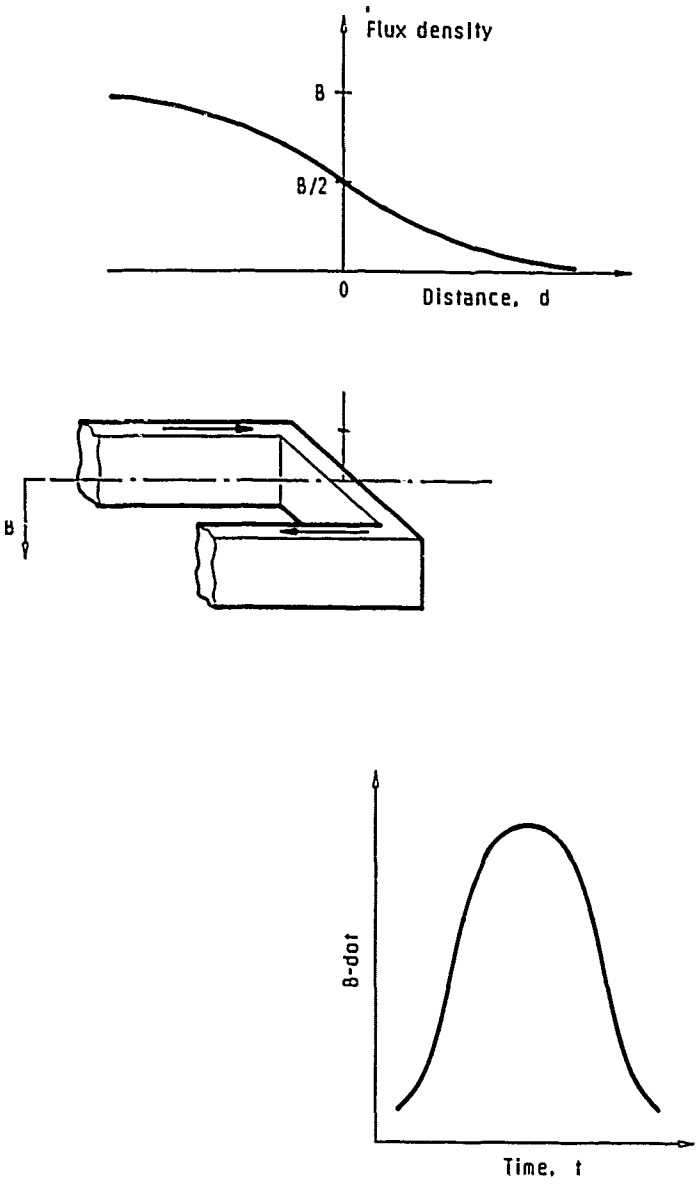

Figure 14 Flux relationships for a simple railgun model.

Plasma velocity for the RIPLAM data was re-evaluated also using first-peak data producing the results of Table 5. The use of first-peak data for deriving plasma velocity produced more uniform values over the separation distance of the three coils. This contrasted with the 'no-change' result for some of the RIPAL 2 data and may reflect an improvement in the coil construction technique. These observations suggest that secondary effects in the coils are more complicated, and more significant, than previously considered.

Table 5 **Plasma velocity for RIPLAM using two methods**

Method	Array coils	Positive Rail 1-2	Positive Rail 2-3	Negative P 1-2	Negative P 2-3
		Velocity (km/s)			
Cross-overs	Incremental	2.3	1.0	1.	1.9
	Overall (1-3)	1.3		1.6	
1st Peaks	Incremental	1.8	1.5	1.7	1.9
	Overall (1-3)	1.6		1.8	

On reviewing all the arguments and the B-dot time data obtained, it is considered that the cross-axis sensitivity of the coils was probably too high. This has occurred despite the extra attention paid to the winding of the array coils for the latter two sets. Therefore the time-of-crossover data was not generally reliable. Consequently, comparative measurements between perturbations on various coils, based on cross-over data, would be generally unreliable.

However the above judgement is not to imply that all the information obtained from the coils was useless. Waveforms can be perturbed by added signals at any point in time. The only time-'distortions' that result are of measurements relative to the base-line cross-over, because of amplitude errors (e.g. a train of time-marker-pulses added to an arbitrary analog waveform retains valid time intervals). Hence time comparisons between a particular coil's waveform features would still be valid. Largely valid too are general waveform effects, since the signal-to-noise ratio is likely to be superior away from the cross-over region. Thus the SUBAC 4 and RIPLAM waveform data cannot be discounted.

In this matter it is worth noting that rail current cannot change very fast. The discharge process is initially dominated by the power supply L and C, and following crowbar, by L to act effectively like a constant current generator. Therefore rail current induced spurious effects are unlikely to be of a high frequency character. Thus one should have reasonable confidence that the higher frequency perturbations about the general background noise were real effects generated by rapid rearrangements within the plasma or on its boundaries.

The final complicating feature of the series of experiments which must be noted is that unfortunately power supply crowbar occurred close to or within the measurement period. For RIPLAM, crowbar appears to have coincided with the coil 3 column transition. The crowbar switch itself was distant from the coils. However it could account for some very high frequency features appearing across all coils simultaneously. The common feature noted in Figure 11 may well be a spurious effect occurring at crowbar initiation. For RIPAL, crowbar was closer to transition of the coil 1 set.

In addition to the data already referred to, there is evidence of a dynamic plasma provided by a study of the waveforms from the bore centre-line B-dot coil 25 mm past the array centre.

Considering the two waveforms in Figure 15, it can be seen that the second halves are noticeably different. This was interpreted as indicating that, for this shot, either the plasma current distribution at the rail boundary was slightly different from that at the centre-line, or the current distribution changed over the coil-separation distance of 17 mm.

It is clear that the coil array to gun-bore separation was less than desirable for confident discrimination of localised rail or plasma-body effects. Nevertheless, with array row-to-row separation of 8 mm for RIPAL and RIPLAM, and 13 mm for edge row centre-line to bore centre-line, the coils would have been able to discriminate rail-specific, isolated, distinctive sub-arc effects. The calculated ratio of outputs from coils in the same column to an arc feature immediately below one side coil and in the centre of that rail is approximately 1.8. The value rises to 2.8 for localised effects at the rail surface near the bore face closest to the coil. On this basis, considering the relative amplitudes of the features identified in Figure 11, there may be other interpretations than the crowbar response attributed earlier.

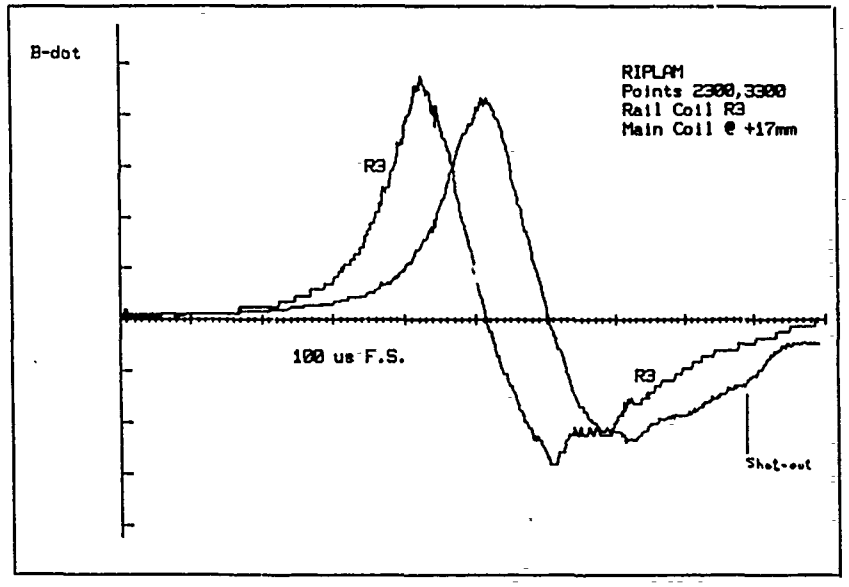

Figure 15 *Waveform from a conventional B-dot coil 25 mm past the array centre-line. A rail-edge coil output is added for comparison.*

Supplementing any evidence from the waveforms was the convincing evidence from rail damage that, during the observed phase of shot-life, the electrical connection between the plasma and the rails was, at least in part if not completely, via an arc structure, and that the arc structure may have been quite different at the two boundary rails.

It is difficult to know whether the perturbations observed on B-dot waveforms were generated by plasma-rail boundary arc effects, or by structures within the body of the plasma, or by a combination of effects, including external influences.

There appeared to be two sorts of perturbation, one being a high-frequency effect typically observed on B-dot first-peaks, and the other being fundamentally a lower frequency effect, typically observed on B-dot second-peaks. The mixture of the two components appeared to be a function of the shot parameters, e.g. plain rails versus rails with aluminium inserts or insulating channels. The slower perturbations may have corresponded to localised variations in conductivity along the plasma length. Non-uniform mixing of fresh plasma material such as metal vapour could produce such an effect.

The finer structures observed are more likely to have had arc-filament or arc-root origins. Since fine structure is as evident on centre-line coils as on bore-edge coils, it is likely that it corresponds to some arc structure in the body of the plasma. One must then consider whether such an arc structure is the same as that generating arc-track damage.

Since the nature of the finer of the two waveform perturbations was highly variable from shot-to-shot, yet for all shots the rails showed extensive arc-track damage, it seems likely that a different arc structure may have existed at the rails to that observed by all B-dot coils. Failure to detect a boundary arc structure could be explained by the presence of a large number of arcs in the boundary structure. Detection would be even more difficult if the boundary arc lengths were very short. The latter would be consistent with the earlier statement that similar detail was observed on all coil waveforms. The coils would need to be much closer to the plasma interface to provide good spatial discrimination of B-dot effects. This would require some ingenuity to implement.

In summary it is suggested that:

1. The small, high frequency waveform perturbations observed around B-dot first peaks were likely to have been associated with some filamentary structure within the front of an essentially diffusely-conducting plasma body, and not with plasma-rail boundary effects. This structure can change significantly over several microseconds.

2. Conduction at the rail boundary was largely if not totally due to an extensive fine-arc-structure (of arc-roots or sub-arcs), with arc lengths being one millimetre or less. (No consideration has been given to the nature of the interface of the boundary-arc structure and the bulk of the plasma).

3. It is likely that plasma current distribution was different both across and along a rail, and at each rail.

4. At the current levels used in the experiments reported here, a significant portion of the rail surface takes little part in the actual plasma-to-rail current conduction process.

5. Coarse perturbation in and following the second B-dot peak reflect variations in uniformity of current distribution in the 'tail' of the plasma. The effect may be a function of the parameters of the particular firing, e.g. one firing which used rails with aluminium inserts appeared to generate a smoother plasma tail than the copper-only firings.

6. The instrumentation used was unable to detect any effects supporting the arc-root movement hypothesis for the plasma-rail interface.

7. The presence of a large 'cross-axis' signal around the time of zero-cross-over increases the need for a coil design offering low cross-axis-sensitivity, i.e. low sensitivity of a coil to flux components perpendicular to the coil axis.

Finally, the greatest difficulty in pursuing plasma structure or boundary investigations based on B-dot probing, appears likely to be the construction and verification of suitable B-dot coils.

10. Conclusion

An experiment was conducted to look for the presence of arc-roots in railgun plasmas and, if observed, to look for evidence of their relative movement with respect to the plasma bulk.

The data gathered from an array of coils near the rails did not provide any convincing evidence for the existence and movement of arc-roots at the plasma-rail boundaries. However, rail damage effects were consistent with the existence of rapidly changing and rail-unique small arc-root structures. Observed electrical effects were not inconsistent with such a view. Experimental observations do support the notion of a rapidly changing sub-structure within the plasma armature body. Clearly the plasma-rail interface is a highly complex region still requiring considerable study. Much also remains to be learnt about effects within the plasma body.

11. Acknowledgements

I wish to acknowledge the contribution of Dr Richard Marshall who conceived and devised the original experiment during his stay at MRL as a visiting scientist, the support of Mr G.A. Clark and Mr W.A. Jenkins in the experimental aspects of the work, and the technical assistance of Mr J. Ferrett and Mr G. Harrison.

12. References

1. Jamison, K.A. and Burden, H.S. (1983). *A laboratory arc-driven railgun* (Report ARBRL-TR-02502). Maryland: Ballistic Research Laboratory, AMCCOM Aberdeen Proving Ground.

2. Bedford, A.J. (1984). Rail damage in a small-calibre railgun. *IEEE Transactions on Magnetics*, Vol. MAG-20, No. 2.

3. Marshall, R.A. (1985). The nature of the plasma armature in a railgun. *15th AINSE Plasma Physics Conference*, Lucas Heights Research Laboratories, NSW, Australia.

4. Batteh, J.H. and Powell, J.D. (1984). Analysis of plasma arcs in arc-driven railguns. *IEEE Transactions on Magnetics*, Vol. MAG-20, No. 2.

5. Bedford, A.J., Clark, G.A. and Thio, Y.C. (1983). *Experimental electromagnetic launchers at MRL (U)* (Report MRL-R-894). Maribyrnong, Vic.: Materials Research Laboratory.

6. Macintyre, I.B. (1984). High speed photographic analysis of railgun plasmas. *16th International Congress on High Speed Photography and Photonics*, SPIE Vol. 491.

7. Stainsby, D.F. and Sadedin, D.R. (1987). *Experiments with a small injected railgun (U)* (Report MRL-R-1055). Maribyrnong, Vic.: Materials Research Laboratory.

DOCUMENT CONTROL DATA SHEET

REPORT NO.	AR NO.	REPORT SECURITY CLASSIFICATION
MRL-R-1057	AR-005-136	Unclassified

TITLE

An experimental study of plasma structure in a small railgun

AUTHOR(S)

D.F. Stainsby

CORPORATE AUTHOR

DSTO Materials Research Laboratory
PO Box 50
Ascot Vale Victoria 3032

REPORT DATE	TASK NO.	SPONSOR
August, 1990		

FILE NO.	REFERENCES	PAGES
G6/4/8-3221	7	32

CLASSIFICATION/LIMITATION REVIEW DATE

CLASSIFICATION/RELEASE AUTHORITY
Chief, Underwater Systems Division

SECONDARY DISTRIBUTION

Approved for public release

ANNOUNCEMENT

Announcement of this report is unlimited

KEYWORDS

Boundary layer
Plasma propulsion
Railgun accelerators

SUBJECT GROUPS

ABSTRACT

Miniature B-dot coils were used to probe the current in the plasma boundaries at both the positive and negative rails in a small railgun. Waveforms from a row of three coils at each rail were examined for evidence of the existence of time-ordered fine structure effects within the plasma boundary. No such order was detected. However, spatially correlated effects were observed and these were attributed to rapidly changing filamentary structure in the plasma. The polarity-reversal, or cross-over characteristics, of the B-dot waveforms showed anomalous features. Possible explanations are discussed. Evidence from rail damage is presented supporting the view that the rail-plasma boundary is associated with a number of complex processes and that localized irregularities in the B-dot waveforms should be expected.